

DEVELOPMENT OF A MOLECULAR MECHANICS FORCE FIELD FOR CLAYS I. STRUCTURE AND IR SPECTRUM OF KAOLINITE

Alan G. Stupp, John B. Nicholas, Kathleen A. Carrado,
Glenn L. Keldsen, and Randall E. Winans
Chemistry Division, Building 200
Argonne National Laboratory
Argonne, IL 60439

Keywords: Molecular Mechanics, Force Field, Clays, Kaolinite

INTRODUCTION

The use of layered inorganic silicate clays as catalysts remains technologically vital to industry¹. It is therefore important to understand the chemistry involved with these compounds. Comprehension of the structure and dynamics of the material, how other ions and molecules interact with the clay, and the reaction mechanisms involved in the catalysis process are all critical issues. Molecular modeling techniques, encompassing energy minimization or molecular mechanics², normal mode analysis, molecular dynamics, and computer graphics, is a valuable tool for examination of these properties.

The purpose of this work was to apply molecular modeling techniques to the study of silicate clays to determine their structure and dynamics. Previous studies of related materials^{3,4,5} suggested that the results obtained would be of sufficient accuracy to compare to experiment. In addition, more accurate, *ab initio* calculations on such large molecules are nearly impossible at the present time, even on large supercomputers.

THEORETICAL METHODS

Atomic Coordinates

Our modeling efforts begin with kaolinite, an important and common clay mineral from the Kaolin or Kandite group⁶. This class of minerals is made up of a single Si(Al, Fe)-O tetrahedral sheet linked to a single Al(Mg, Fe)-OH octahedral sheet in regular succession, as displayed in Figure 1. As such, these clays are also called 1:1 minerals.

Atomic coordinates were taken from Young and Hewat's Rietveld refinement⁷ of both X-ray and neutron powder diffraction data. This refinement was chosen because Young and Hewat measured the most crystalline material available and gave definitive positions for the inner-hydroxyl hydrogen atoms. A space group of P1 was used for this refinement and the resulting cell parameters appear in Table I. The reported values, which were used for this model, must however be viewed with some caution, since aspects^{7,8,9} about the actual space group and cell parameters are still being questioned, sixty years after the idealized structure was proposed by Pauling¹⁰. The major argument about the structure seems to be whether or not the hydrogen atom positions of the inner-hydroxyls are c-face centered. The reason for many of these disputes is that available crystals of kaolinite have not been sufficiently large or coherent enough to allow good single crystal analysis¹¹.

Peak assignments for comparison to the theoretical infrared (IR) spectrum of kaolinite were taken from a compendium of data on layered materials¹². Several infrared spectra for kaolinite from different parts of the world and of different purities are contained in this source. To remain consistent with Young and Hewat⁷, who used kaolinite from Keokuk, Iowa, the IR spectrum of the Keokuk kaolinite was used.

Simulation

The simulation system was formed by several replications of the unit cell. A 4x2x3 arrangement giving a cell containing 816 atoms and having the dimensions 19.89Å x 17.86Å x 22.16Å was used for the molecular dynamics calculations. Periodic boundary conditions were used to simulate the effects of an infinite lattice framework. The non-bonded interatomic interactions were evaluated for all atoms within a cut-off radius of 8.93Å.

Non-bonded Lennard-Jones and electrostatic interactions were not calculated for atoms that were bonded (1-2 interactions) or for atoms that were involved in a bond angle (1-3 interactions), because these are accounted

for by the bond stretch and bond angle bend potentials. The method of conjugate gradients¹³ was used for the energy minimization routines. The molecular dynamics calculations were done using the "leap-frog" algorithm¹⁴ to integrate the equations of motion.

Force Field

Molecular modeling techniques that are based on classical mechanics require a force field to describe inter- and intra-molecular interactions. The force field used in this work is represented by the sum of potential energy terms:

$$V = V_s + V_\theta + V_{nb}$$

where V_s is the potential caused by bonds stretching from their equilibrium positions, V_θ is the potential related to the bending of bond angles from their equilibrium positions, and V_{nb} is the potential associated with non-bonding interactions.

Force parameters used in the potential energy terms can be calculated several ways. Quantum mechanical calculations on small molecules that mimic the clay structure can be used to determine force constants, equilibrium geometries, and charge densities. Fitting the force parameters to existing experimental data, such as IR frequencies and crystal structures, is possible and was used to help define some of the force field parameters in this work. The equilibrium values can also be varied over a small range and plotted versus the difference in potential energies of the original structure and its minimized counter-part. This method was also used for some of the force parameters in this work.

The bond stretch potentials in the force field were based on a simple harmonic potential:

$$V(r) = (K_r/2)(r-r_{eq})^2$$

where r is the interatomic distance between atoms, r_{eq} is the equilibrium bond length and K_r is the bond stretching force parameter.

Bond angle bends were also modeled after a simple harmonic potential:

$$V(\theta) = (K_\theta/2)(\theta-\theta_{eq})^2$$

where θ is the bond angle bend, θ_{eq} is the equilibrium bond angle and K_θ is the bond angle bend force constant.

The non-bonded interactions considered were of two types. The first was the Lennard-Jones 6-12 potential

$$V(r) = B/r^{12} - A/r^6$$

where A and B are Lennard-Jones parameters taken from the MM2¹⁵ force field. The second non-bonded interaction accounted for was that of electrostatic interactions. These were modeled by a Coulomb potential:

$$V(r) = q_i q_j / \epsilon r$$

where q_i and q_j represent the charges of the atoms and ϵ is the dielectric constant. The electrostatic forces are of longer range and can be more important than the Lennard-Jones terms.

RESULTS AND DISCUSSION

An important test for the accuracy of any force field is its ability to reproduce the experimental crystal structure. Energy minimizations were performed starting with the reported crystal structure of kaolinite. The final structure after minimization was then compared to the original structure using both computer graphics and root mean square (RMS) differences (Table II) for each atomic coordinate. In Figure 2 it can be seen that the minimized geometries are very close to that of the original structure, especially for the heavier silicon and aluminum atoms. The oxygen and hydrogen atoms, which are expected to have greater freedom of movement in the actual compound, account for the major differences between the theoretical and actual crystal coordinates. It is interesting to note that the inner-hydroxyl hydrogens in the minimized structure have assumed a c-centered positioning (pointing in the same direction), which deviate from the original coordinates where they point towards

different layers in the clay. However, this may be caused by the absence of a hydrogen bonding potential in the force field. If this potential is added it may cause the hydroxyl hydrogens to point towards the tetrahedral silicon layer.

Another check for the accuracy of the model force field is the force field's ability to predict the infrared spectrum. This can be done in two ways. Normal mode analysis can be used to determine the frequencies of the vibrations of the molecule. A theoretical infrared spectrum can also be calculated from molecular dynamics. This is done by taking the Fourier transform of the total dipole correlation function¹⁶ calculated from the molecular dynamics trajectory. The intensities obtained by either method are, however, strictly qualitative because the quantum corrections needed to give accurate intensities are impractical for such a large system. The force parameters and equilibrium values used in the theoretical force field are summarized in Table III.

The theoretical and experimental¹² infrared spectra for kaolinite are compared in Figure 3. Very good correlation is found in the 14 to 24 micron region of the spectrum. According to both the literature¹⁷ and to the normal mode calculations carried out on the model structure, the peaks at 19 and 21.5 microns are due to the Si-O bond stretch. The fact that the experimental and theoretical peaks match well indicate that the Si-O parameters are correct. The experimental peak at 14.5 microns is due to the Si-O-Al bond angle bend¹⁷, however, the theoretical peak is at a slightly lower energy value (16 microns). The 8 to 13 micron range of the theoretical spectrum does not clearly exhibit all the major peaks in the experimental IR spectrum, but tentative assignments can be made. The Si-O bond stretch at 9.0 microns is calculated to occur at 8.5 microns and the theoretical peak at 10.2 microns is believed to correspond to the experimental peak at 9.9 microns. This peak, along with the band at 14.5 microns, may be due to the Si-O-Al bond angle vibration. Additional molecular dynamics calculations are being performed to adjust the force constants to achieve agreement with experiment in the 8 to 10 micron region.

CONCLUSION

A force field for the clay kaolinite has been developed that gives good results both for reproducing the experimental crystal lattice structure and the infrared spectrum. A final test for this force field will be its ability to be transferred to other 1:1 layered minerals that contain aluminum, silicon, and oxygen.

ACKNOWLEDGMENTS

The Division of Educational Programs at Argonne National Laboratory is acknowledged for providing full support for AGS. This work was performed under the auspices of the Office of Basic Energy Sciences, Division of Chemical Sciences, U.S. Department of Energy, under contract number W-31-109-ENG-38.

REFERENCES

1. Pinnavaia, T.J.; *Science* **1983**, *220*, 365.
2. Boyed, D.B.; Lipkowitz, K.B. *J. Chem. Ed.* **1982**, *59*, 269-274.
3. van Beest, B.W.H.; Kramer, G.J.; van Santen, R.A. *Phys. Rev. Lett.* **1990**, *64*, 1955-1958.
4. Mabilia, M.; Pearlstein, R.A.; Hopfinger, A.J. *J. Am. Chem. Soc.* **1987**, *109*, 7960-7968.
5. Sander, M.J.; Leslie, M.; Catlow, C.R.A. *J. Chem. Soc. Chem. Comm.* **1984**, 1271.
6. Grim, R.E. *Clay Mineralogy*; McGraw-Hill: New York, **1968**, pp. 35-38.
7. Young, R.A.; Hewat, A.W.; *Clays Clay Miner.* **1988**, *36*, 225-232.
8. Adams, J.M. *Clays Clay Miner.* **1983**, *31*, 352-356.
9. Thompson, J.G.; Withers, R.L. *Clays Clay Miner.* **1987**, *35*, 237-239.
10. Pauling, L. *Proc. Nat. Acad. Sci.* **1930**, *16*, 123-129.
11. Giese, R.F. *Reviews in Mineralogy*, Vol. 19, S.W. Bailey, Ed., **1988**, pp 30-35.
12. van der Marel, H.W.; Beutelspacher, H. *Atlas of Infrared Spectroscopy of Clay Minerals and their Admixtures*; Elsevier Scientific: New York, **1976**, pp 65.
13. Gunsteren, W.F.V.; Karplus, M.J. *J. Comp. Chem.* **1980**, *11*, 266-274.
14. Hockney, R.W. *Methods Comput. Phys.* **1970**, *9*, 136-211.
15. Allinger, N.L.; Yuh, Y.H.; Lii, J.H. *J. Am. Chem. Soc.* **1989**, *111*, 8551-8566.
16. Berens, P.H.; Wilson, K.R. *J. Chem. Phys.* **1981**, *74*, 4872-4882.
17. van der Marel, H.W.; Beutelspacher, H. *Atlas of Infrared Spectroscopy of Clay Minerals and their Admixtures*; Elsevier Scientific: New York, **1976**, pp 57.

Table I. Lattice parameters of kaolinite from Young and Hewat⁷.

$a = 5.1497 \text{ \AA}$	$b = 8.9351 \text{ \AA}$	$c = 7.3855 \text{ \AA}$
$\alpha = 91.93^\circ$	$\beta = 105.04^\circ$	$\gamma = 89.79^\circ$

Table II. Room mean square (RMS) differences between X-ray crystal data and minimized structure of kaolinite.

RMS(x): 0.024	RMS(y): 0.016	RMS(z): 0.018
---------------	---------------	---------------

Table III. Force parameters and equilibrium values used in the calculated force field of kaolinite.

O(1): oxygen in silicon-oxygen rings
O(2): oxygen between silicon and aluminum layers
O(3): oxygen in bridging hydroxyls
O(4): oxygen in terminal hydroxyls

<u>BOND TYPE</u>	<u>FORCE PARAMETER (mdyne/\AA)</u>	<u>r_{eq} (\AA)</u>
Al-O(2)	2.60	1.93
Al-O(3,4)	2.80	1.77
Si-O(1)	4.15	1.65
Si-O(2)	4.15	1.63

<u>BOND TYPE</u>	<u>FORCE PARAMETER (mdyne/deg)</u>	<u>θ_{eq} (°)</u>
O(1)-Si-O(1)	0.96	106.5
O(1)-Si-O(2)	0.96	106.5
O(2)-Al-O(2)	0.90	90.0
O(2)-Al-O(3)	0.90	90.0
O(3)-Al-O(3)	0.90	90.0
Si-O(1)-Si	0.40	146.5
Al-O(2)-Al	0.10	138.0
Al-O(2)-Si	0.40	135.0
Al-O(3)-Al	0.40	138.0
Al-O(4)-H	0.15	120.0

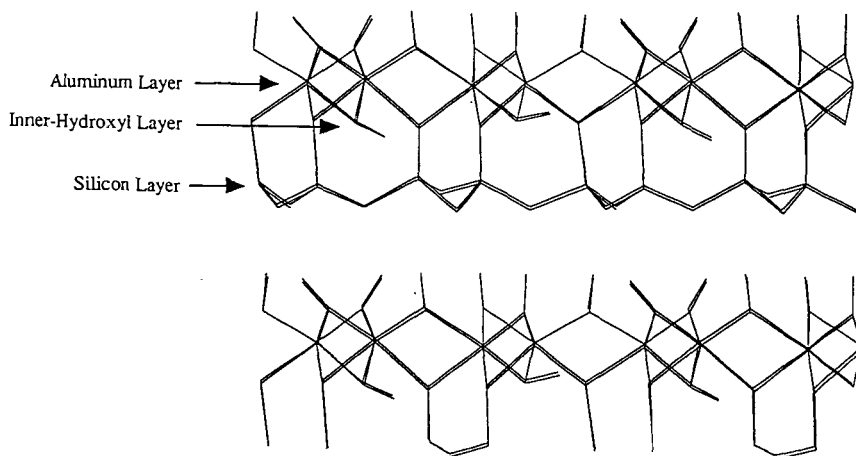


Figure 1. X-ray crystal structure of a $2 \times 2 \times 2$ lattice of kaolinite

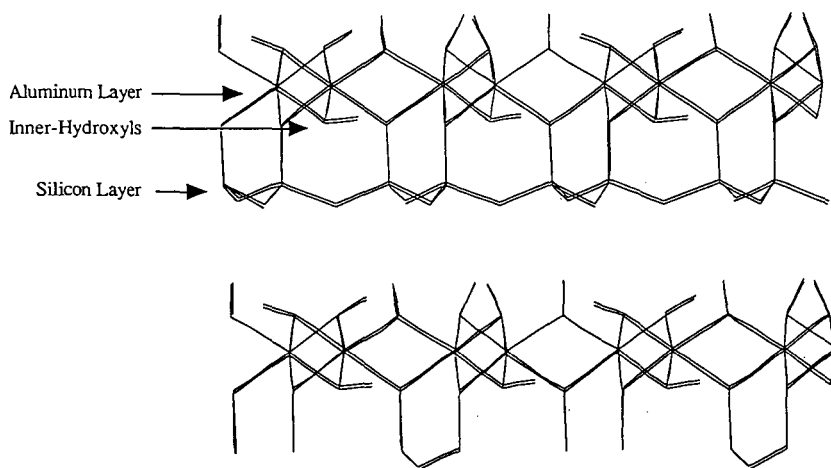


Figure 2. Minimized structure of kaolinite

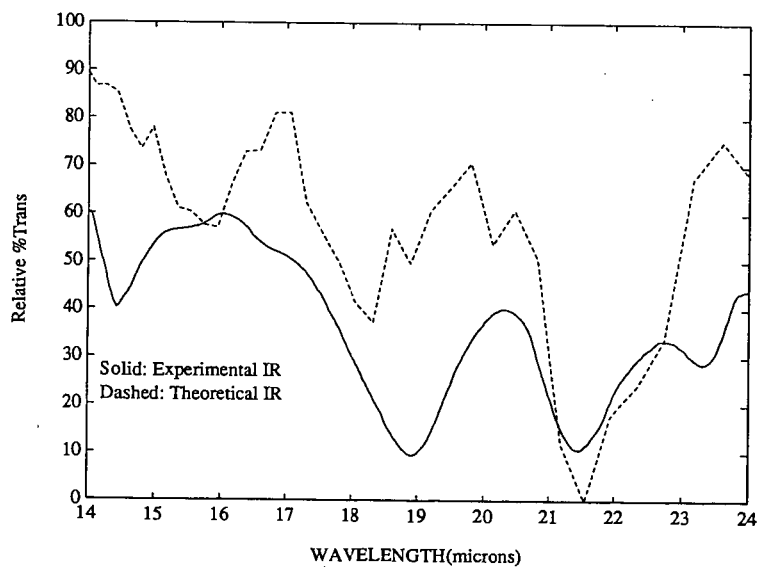
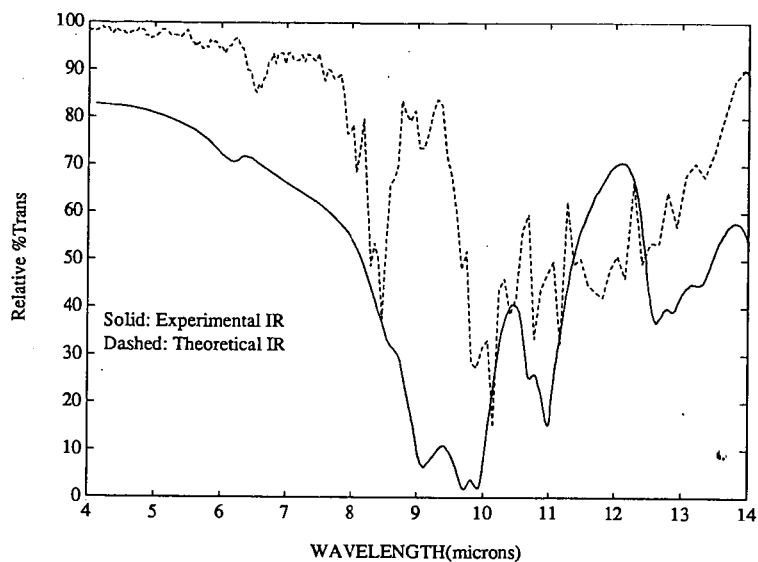


Figure 3. Comparison of theoretical and experimental infrared spectra of kaolinite